

A Novel Texture Descriptor for Texture Image Retrieving

Chung-Ming Kuo, Nai-Chung Yang, Shen-Cha Tseng, Meng-Tso Chen

Department of Information Engineering
I-Shou University, Taiwan, R.O.C
*Corresponding author: kuocm@isu.edu.tw

Received January 2018; revised August 2018

ABSTRACT. *The techniques of content-based image retrieval (CBIR) has been widely applied to multimedia databases. In this paper, we will propose a new texture descriptor for texture image retrieval. The new method Range Local Binary Pattern (RLBP) to address the drawbacks of conventional local binary patterns (LBP) and fuzzy local binary patterns (FLBP). The LBP algorithm is a very simple method, which labels each pixel according to its neighborhood distribution. The main drawback is very noise sensitive. Therefore, the FLBP algorithm was proposed to improve the weakness, it defines the characters of the fuzzy region and uses statistics method to extract texture features. However, the FLBP algorithm consumes high computational cost. To reduce the complexity, we proposed co-occurrence range local binary patterns (Co-RLBP) methods to model the spatial correlation and then obtain adequate information to increase the description accuracy. Experimental results indicate that the proposed method achieves satisfactory performance for texture image retrieval.*

Keywords: Texture descriptor, Image retrieval, Range local binary patterns.

1. **Introduction.** In recent years, digital images and videos are wildly used in various applications. The use of low-level features by the content-based image retrieval (CBIR) to retrieve relevant information from image databases becomes more and more important [1]-[4]. Texture is one of the most important features for image retrieval. Although there is no formal definition for texture, it could be defined intuitively as a structure composed of a large number of similar patterns [5][6]. Several of the recently proposed texture descriptors have been developed for extracting features from images. For instance, several texture-based techniques for CBIR have been developed to demonstrate the effectiveness of the integrated systems [7]-[10].

To support image retrieval, various methods for representation of textures have been proposed for various applications. Generally, the feature selection has to be performed for each specific application to decide which one should be used. In other words, proper choice of the right features from the texture leads to a successful retrieval. For example, MPEG-7 specifies three texture descriptors including homogeneous texture descriptor (HTD), texture browsing descriptor and edge histogram descriptor to describe the texture contents of multimedia [1]-[4] for different applications.

In order to capture textures, model based methods have been wildly used for extracting textural properties such as uniformity, coarseness, roughness, regularity and directionality. In general, these methods captured micro textures well, but they maybe fail with regular and inhomogeneous textures [5][6]. To overcome this difficulty, we propose a novel texture

model based on local difference distributions of pixels in images [7]-[12]. In this paper, we will propose a novel LBP feature representation approach, which is not only robust for noise but also with strong spatial correlation. Finally, extensive simulations for various images are conduct to evaluate the performance. In the following Sections, the detail discussion will be given. However, the phase 1 is not the main issue in this paper. The paper is organized as follows. In section 2, we describe the ideas about texture feature extraction and description. The proposed model for extracting the feature is explained in Section 3. A discussion and comparison is made in Section 4. Finally, a short conclusion is presented in Section 5.

2. Texture feature extraction and description. Local binary pattern (LBP) is originally proposed for texture image segmentation [24]. Although LBP has been widely used in many applications, it has two inherent problems need to be addressed. First, the value of LBP is not a quantity, but it represents a local distribution. Therefore, the similar value does not imply the similar distribution. Second, the binarization of LBP is a hard decision by thresholding center pixel, it is very noise sensitive. According to the drawbacks mentioned above, we will propose a novel range local binary pattern (RLBP) to address the problem of noise interference. To consider the spatial correlation, we also develop a new representation, which is inspired by Haralick’s co-occurrence matrix [5]. We present CO-LBP (co-occurrence local binary patterns) and CO-RLBP (co-occurrence range local binary patterns) methods to model the spatial correlation and then obtain adequate information to increase the diagnostic accuracy. In our work, we define an ambiguous range for the LBP thresholding. Let T be the ambiguous range, Eq. (1) and (2) are the calculation of RLBP.

$$d_n(i, j) = \begin{cases} 1 & \text{if } p_n \geq p_{center} + T \\ 0 & \text{if } p_{center} - T < p_n < p_{center} + T, n \in (i, j)_{3 \times 3} \\ -1 & \text{if } p_n \leq p_{center} - T \end{cases} \quad (1)$$

$$RLBP(i, j) = \sum_{n=0}^7 d_n(i, j) \cdot 2^n \quad (2)$$

where p_n is the pixels in 3×3 mask, p_{center} is the center pixel in 3×3 mask, is the weighting value in mask and $d_n(i, j)$ is the decision results. The histogram of LBP can be expressed as

$$H_{RLBP} = \langle h_{RLBP}(k) \rangle \quad k = -255, -254, \dots, 255 \quad (3)$$

$$h_{RLBP}(k) = \frac{1}{M \times N} \sum_{i=0}^M \sum_{j=0}^N \delta(RLBP(i, j) - k) \quad k = -255, -254, \dots, 255 \quad (4)$$

$$H_{RLBP} = \sum_{k=-255}^{255} h_{RLBP}(k) = 1 \quad k = -255, -254, \dots, 255 \quad (5)$$

, where M and N are the height and width of texture image, k is the RLBP value, $RLBP(i, j)$ is the RLBP value in (i, j) and $h_{RLBP}(k)$ is the normalized distribution of the k^{th} bin. The most important difference in LBP and RLBP is the consideration of noise introduced in ultrasound image. Basically, in conventional LBP, it depends only on the comparisons between central pixel and its surrounding pixels according to their magnitude. In other words, the comparison has only two possible results, larger or smaller. However, due to the noise interference, the pixel value close to the central pixel may cause

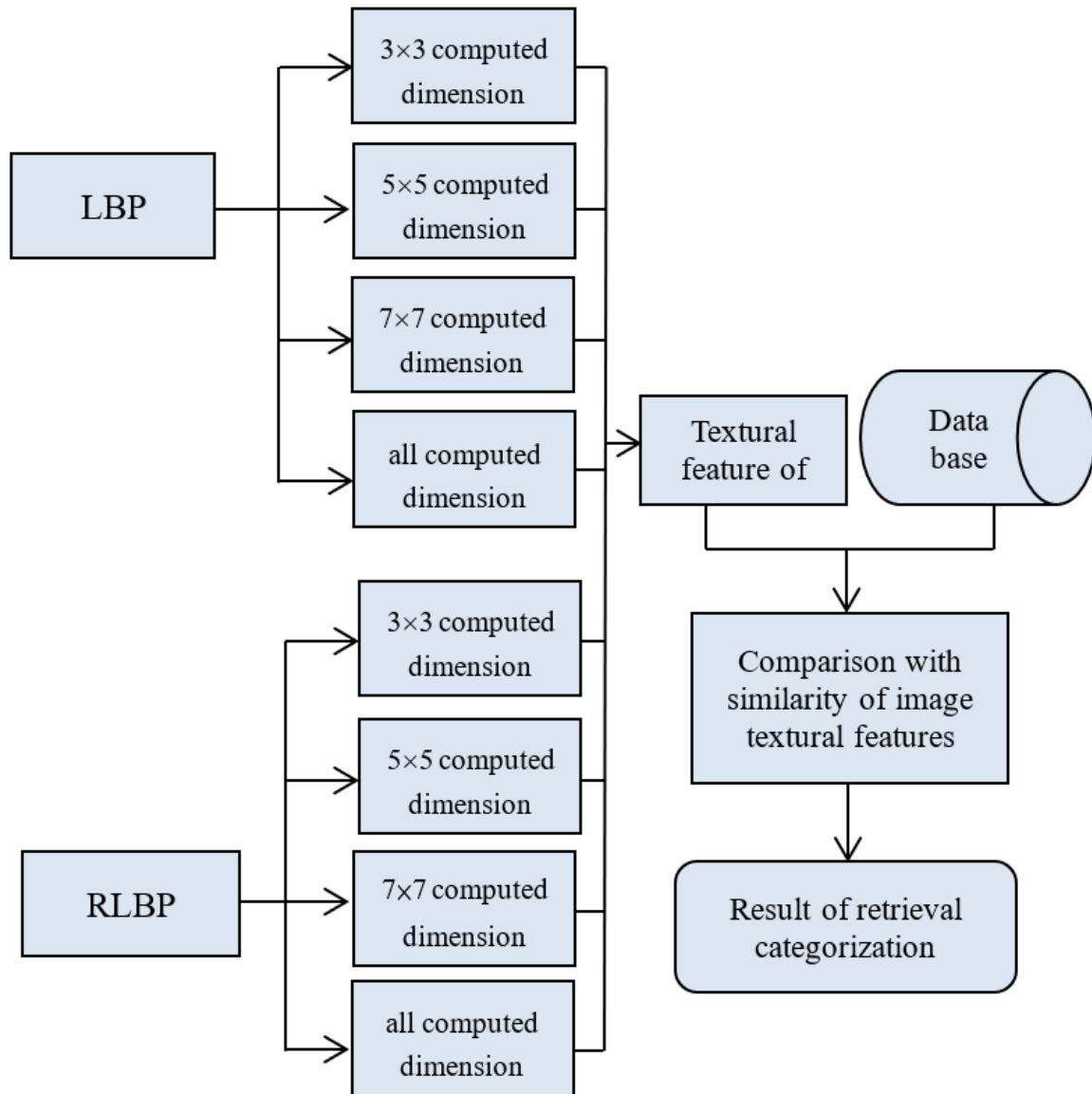


FIGURE 1. The flow chart of feature texture image retrieval system

the wrong LBP decision. Therefore, using the LBP, it is easy to make mistake for noisy images. RLBP, on the other hand, considers the noisy effect and create "0" to represent the value which is close to the ambiguous range of central pixel value. RLBP provides two advantages. First, it can reduce wrong decision. Second, it can capture the precise LBP for statistical analysis. Using the RLBP, it can provide the convincing analytical result in the description of texture feature under the condition of noisy effect. Therefore, we can expect that the proposed feature representation will effectively address the noise interference in image.

3. The Proposed LBP and RLBP representation. In this section, we will propose a novel texture feature descriptor based on local binary pattern (LBP). The new texture descriptor addresses the drawbacks of conventional LBP such as noise sensitive and spatial correlation. We will evaluate the effectiveness of new descriptor by using image retrieval system as shown in Fig. 1.

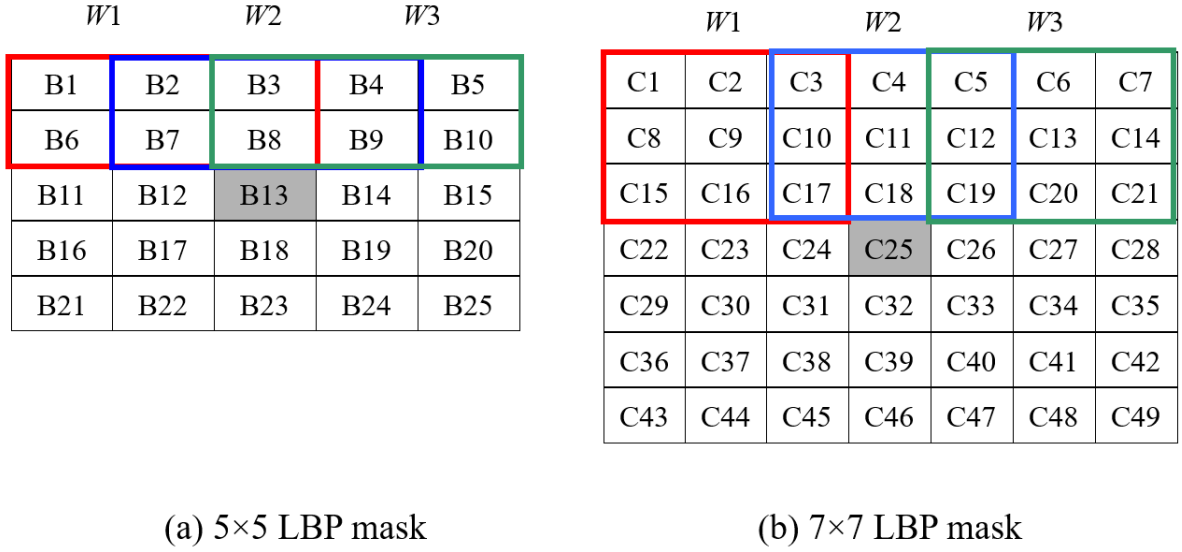


FIGURE 2. Deference size of LBP masks

To consider the texture distribution more comprehensively, we improve the LBP and RLBP by using various dimensions to compute LBP. The new spatial dimensions for LBP computation are with mask 3×3 , 5×5 and 7×7 , and be expressed as: $\{LBP^3(i, j), LBP^5(i, j), LBP^7(i, j)\}$, respectively. For $LBP^3(i, j)$, the computation is the same as conventional LBP. In order to satisfy the computation rule, the mask of $LBP^5(i, j)$ or $LBP^7(i, j)$ is simplified from a 5×5 or 7×7 to 3×3 ; the mask and simplification scheme are shown in Fig. 2, Eq.(6) and (7), respectively.

$$LBP^5(i, j) = \begin{bmatrix} W1 \\ W2 \\ W3 \\ W4 \\ W6 \\ W7 \\ W8 \\ W9 \end{bmatrix}, \quad (6)$$

$$\begin{aligned}
 W1 &= \frac{B1 + B2 + B3 + B6 + B7 + B8}{6} \\
 W2 &= \frac{B2 + B3 + B4 + B7 + B8 + B9}{6} \\
 W3 &= \frac{B3 + B4 + B5 + B8 + B9 + B10}{6} \\
 W4 &= \frac{B6 + B7 + B11 + B12 + B16 + B17}{6} \\
 W6 &= \frac{B9 + B10 + B14 + B15 + B19 + B20}{6} \\
 W7 &= \frac{B16 + B17 + B18 + B21 + B22 + B23}{6} \\
 W8 &= \frac{B17 + B18 + B19 + B22 + B23 + B24}{6} \\
 W9 &= \frac{B18 + B19 + B20 + B23 + B24 + B25}{6}
 \end{aligned}$$

$$LBP^7(i, j) = \begin{matrix} W1 \\ W2 \\ W3 \\ W4 \\ W6 \\ W7 \\ W8 \\ W9 \end{matrix}, \begin{matrix} W1 = \frac{C1 + C2 + C3 + C8 + C9 + C10 + C15 + C16 + C17}{9} \\ W2 = \frac{C3 + C4 + C5 + C10 + C11 + C12 + C17 + C18 + C19}{9} \\ W3 = \frac{C5 + C6 + C7 + C12 + C13 + C14 + C19 + C20 + C21}{9} \\ W4 = \frac{C15 + C16 + C17 + C22 + C23 + C24 + C29 + C30 + C31}{9} \\ W6 = \frac{C19 + C20 + C21 + C26 + C27 + C28 + C33 + C34 + C35}{9} \\ W7 = \frac{C29 + C30 + C31 + C36 + C37 + C38 + C43 + C44 + C45}{9} \\ W8 = \frac{C31 + C32 + C33 + C38 + C39 + C40 + C45 + C46 + C47}{9} \\ W9 = \frac{C33 + C34 + C35 + C40 + C41 + C42 + C47 + C48 + C49}{9} \end{matrix} \quad (7)$$

3.1. **Co-occurrence representation of LBP.** We use the concept of co-occurrence matrix to express the spatial relationship of LBP. According to the description of co-occurrence matrix feature, we can clearly identify the relationship of spatial distribution between two texture features. In order to achieve the co-occurrence representation, the conventional LBP mask is decomposed into two sub-masks i.e., "cross" and "corner". As calculation of LBP, the value of each sub-mask is given in Eq. (8) and (9).

$$c_n^+ = \begin{cases} 1 & \text{if } p_n \geq p_{center} \\ 0 & \text{if } p_n < p_{center} \end{cases} \quad (8)$$

$$LBP^+(i, j) = \sum_{n=0}^3 c_n^+ \cdot 2^n \quad (9)$$

where LBP^+ is the LBP value for cross LBP, P_n is the pixels in 3×3 mask, P_{center} is the center pixel in 3×3 mask, 2^n is the weighting value in mask and c_n^+ is the decision results. The sub-mask for corner is expressed as follows. And the definition is the same as in sub-mask in cross:

$$g_n^\times = \begin{cases} 1 & \text{if } p_n \geq p_{center} \\ 0 & \text{if } p_n < p_{center} \end{cases} \quad (10)$$

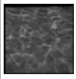

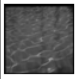
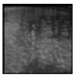


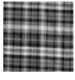










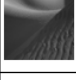







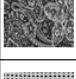
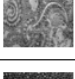
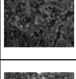
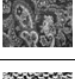
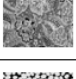
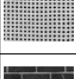
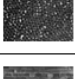
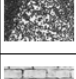
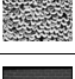
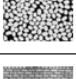





$$LBP^\times(i, j) = \sum_{n=0}^3 g_n^\times \cdot 2^n \quad (11)$$

where LBP^\times is the LBP value for corner LBP, and g_n^\times is the decision results. The histogram of LBP can be expressed as:

$$h_{LBP}^+(k) = \frac{1}{M \times N} \sum_{i=0}^M \sum_{j=0}^N \delta(LBP^+(i, j) - k) \quad k = 0, 1, \dots, 15 \quad (12)$$

$$h_{LBP}^\times(k) = \frac{1}{M \times N} \sum_{i=0}^M \sum_{j=0}^N \delta(LBP^\times(i, j) - k) \quad k = 0, 1, \dots, 15 \quad (13)$$

TABLE 1. Eight sets of test texture images

Sub-class \ Main-class	1	2	3	4	5
water					
clothes					
line					
desert					
rock					
pattern					
spot					
brick					

$$\sum_{k=0}^{15} h_{LBP}^+(k) = 1 \quad k = 0, 1, \dots, 15 \tag{14}$$

$$\sum_{k=0}^{15} h_{LBP}^\times(k) = 1 \quad k = 0, 1, \dots, 15 \tag{15}$$

where M and N are the height and width of texture image and $h_{SS}(k)$ is the normalized distribution in k^{th} bin. For RLBP, we can define similar expressions except the symbols. We briefly summarize the equations of RLBP as follows without further explanations.

$$c_n^+ = \begin{cases} 1 & \text{if } p_n \geq p_{center} + T \\ 0 & \text{if } p_{center} - T < p_n < p_{center} + T \\ -1 & \text{if } p_n \leq p_{center} - T \end{cases} \tag{16}$$

$$RLBP^+(i, j) = \sum_{n=0}^3 c_n^+ \cdot 2^n \tag{17}$$

$$g_n^\times = \begin{cases} 1 & \text{if } p_n \geq p_{center} + T \\ 0 & \text{if } p_{center} - T < p_n < p_{center} + T \\ -1 & \text{if } p_n \leq p_{center} - T \end{cases} \tag{18}$$

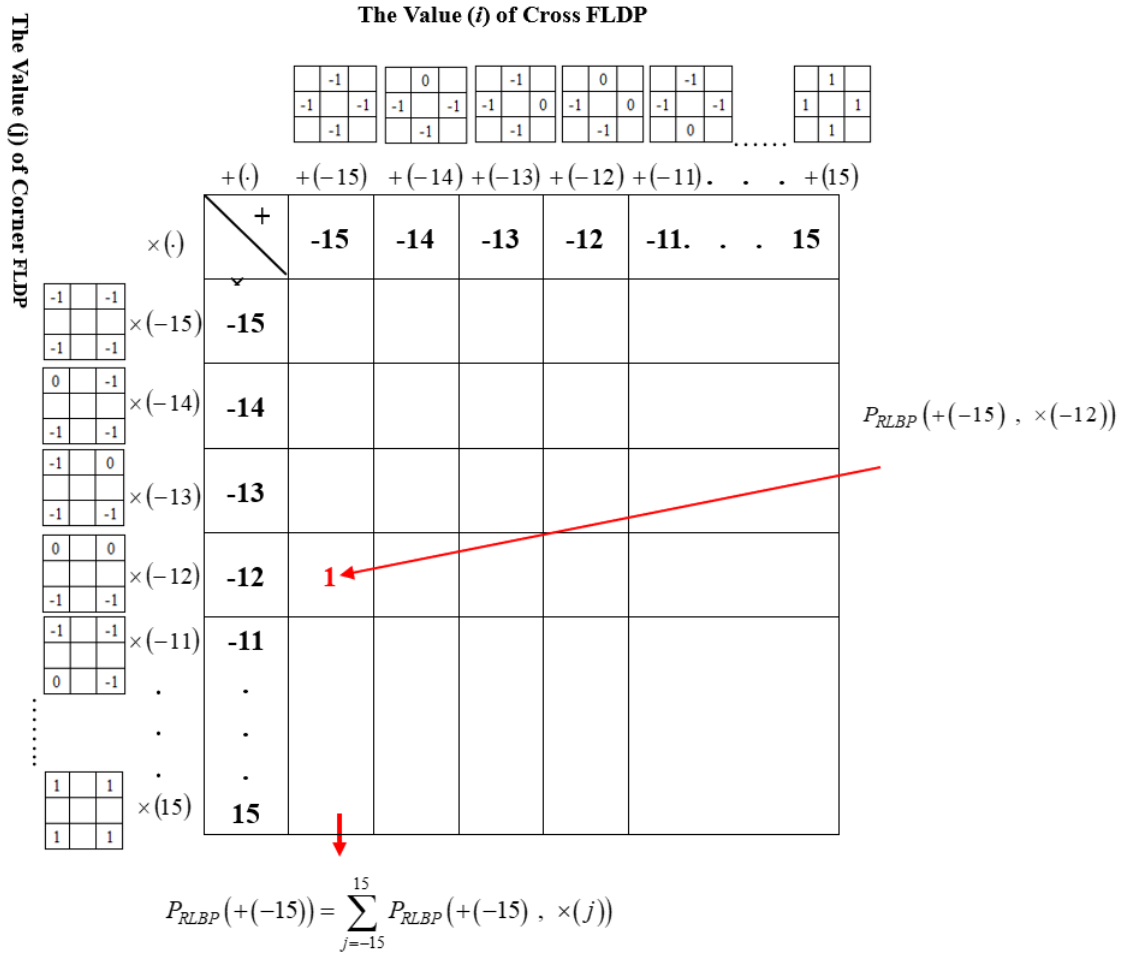


FIGURE 3. Co-occurrence representation of RLBP

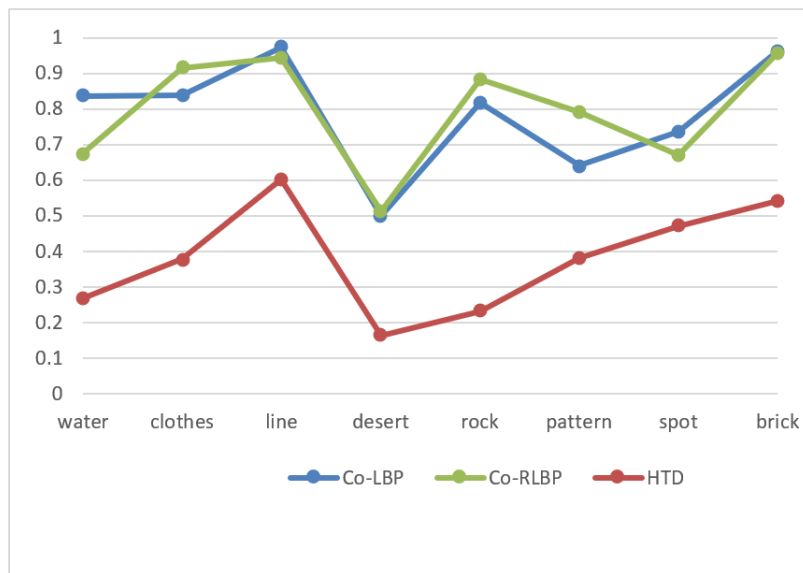


FIGURE 4. Comparisons with ARR for three methods

$$RLBP^\times(i, j) = \sum_{n=0}^3 g_n^\times \cdot 2^n \tag{19}$$

$$h_{RLBP}^+(k) = \frac{1}{M \times N} \sum_{i=0}^M \sum_{j=0}^N \delta(RLBP^+(i, j) - k) \quad k = -15, -14, \dots, 15 \tag{20}$$

$$h_{RLBP}^\times(k) = \frac{1}{M \times N} \sum_{i=0}^M \sum_{j=0}^N \delta(RLBP^\times(i, j) - k) \quad k = -15, -14, \dots, 15 \tag{21}$$

$$\sum_{k=-15}^{15} h_{RLBP}^+(k) = 1 \quad k = -15, -14, \dots, 15 \tag{22}$$

$$\sum_{k=-15}^{15} h_{RLBP}^\times(k) = 1 \quad k = -15, -14, \dots, 15 \tag{23}$$

Once the LBP values for each types are calculated, we define a two dimensional matrix to record the statistics of LBP. Let the row and column represent the ‘‘cross’’ and ‘‘corner’’ features, respectively. For simplicity the symbol $+(i)$ and $\times(j)$ are used to represent the value of $LBP^\times = i$ and value of $LBP^+ = j$ respectively. For example, $P_{LBP}(+(0), \times(3))$ means the total number with the LBP^\times value 0 and LBP^+ value 3 in texture images. Therefore, in same column all elements are with same cross distribution, and in same row all elements are with same corner distribution. Therefore, the elements of co-occurrence matrix can be expressed as

$$P_{LBP}(i, j) = \{(+_{LBP}(i) \text{ and } \times_{LBP}(j)) ; 0 \leq i \leq 15 \text{ and } 0 \leq j \leq 15\} \tag{24}$$

$$P_{RLBP}(i, j) = \{(+_{RLBP}(i) \text{ and } \times_{RLBP}(j)) ; -15 \leq i \leq 15 \text{ and } -15 \leq j \leq 15\} \tag{25}$$

where $P_{LBP}(i, j)$ is the element of co-occurrence matrix of LBP with $LBP^\times = i$ and $LBP^+ = j$, respectively. The definition of $P_{RLBP}(i, j)$ is the same as $P_{LBP}(i, j)$. For a specified cross distribution, the cross LBP for single side non-ambiguous with value 0, can be calculated as,

$$P_{LBP}(+(0)) = \sum_{j=0}^{15} P_{LBP}(+(0), \times(j)) \tag{26}$$

, Using the same procedure, the ambiguous LBP can also be represented as co-occurrence matrix. The new representation of LBP can effectively describe the spatial correlation of local distribution. It is very desired for texture description and classification. In Fig. 3, we show a co-occurrence matrix of RLBP -DS with 3×3 mask, respectively. Because the LBP is calculated from three different dimensional respectively, the LBP from different scale should be merged by weighting sum to obtain the texture feature in various resolution. The calculation of scale 5×5 and 7×7 is simplified to 3×3 according to the calculation rule. Between them the 7×7 is with the highest degree of simplification, therefore the weighting value of 3×3 , i.e., W1, is with the largest value and then 5×5 , i.e., W2, the smallest value is assigned to 7×7 , i.e., W3. The LBP representation can be expressed as

$$CoP_{LBP}(i, j) = 0.6 \times P_{LBP}^{3 \times 3}(i, j) + 0.3 \times P_{LBP}^{5 \times 5}(i, j) + 0.1 \times P_{LBP}^{7 \times 7}(i, j) \tag{27}$$

TABLE 2. Eight sets of test texture images

	Composite image	Source image			
Class 1					
Class 2					
Class 3					
Class 4					
Class 5					
Class 6					
Class 7					
Class 8					
Class 9					
Class 10					

$$\text{CoP}_{\text{RLBP}}(i, j) = 0.6 \times P_{\text{RLBP}}^{3 \times 3}(i, j) + 0.3 \times P_{\text{RLBP}}^{5 \times 5}(i, j) + 0.1 \times P_{\text{RLBP}}^{7 \times 7}(i, j) \quad (28)$$

4. Experimental Results. For performance comparison, the indexes of average retrieval rate (ARR) and average normalized modified retrieval rank (ANMRR) are selected and the higher ARR and lower the ANMRR implies the better performance [2]. In order to evaluate the retrieval effectiveness of the proposed methods, experiments have been conducted based on our database. The database collects 800 photographs. Each photograph is digitized on a 100×100 pixel image with resolution of 256 gray levels. For similarity-based retrieval, the database has been classified to 8 groups including brick, cloth, etc. The final classification is shown in Table 1.

In addition, we create 10 classes of composite images as shown in Table 2. Each class has 10 composite images, and each composite image in a class is consisted of same source images. As shown in Table 2, the left image is composite image, and the followed four images are source images.

In our experiments, all the 900 images have been used as queries for testing the retrieval effectiveness. In the following, we evaluate the performance using two different experiments.

TABLE 3. The performance comparisons for different methods

methods Classes	Co-LBP		HTD		Proposed method (Co-RLBP)	
	ARR	ANMRR	ARR	ANMRR	ARR	ANMRR
water	0.837	0.219	0.269	0.778	0.675	0.356
clothes	0.838	0.2	0.378	0.686	0.916	0.109
line	0.974	0.137	0.602	0.621	0.944	0.136
desert	0.501	0.498	0.165	0.852	0.513	0.487
rock	0.818	0.194	0.233	0.801	0.884	0.131
pattern	0.641	0.383	0.381	0.683	0.792	0.246
spot	0.736	0.26	0.472	0.614	0.67	0.32
brick	0.961	0.05	0.541	0.52	0.956	0.058
Average	0.788	0.242	0.38	0.694	0.793	0.23

Experiment 1. Similarity retrieval for texture To evaluate the similarity retrieval, extensive experiments have been studied for comparison the performance of homogeneous texture descriptor (HTD), conventional local binary pattern (LBP) and proposed RLDP. Table 3 and Table 4 show the detail results for ARR and ANMRR, respectively.

Consider the evaluation by ARR, where a high value represents high retrieval performance. In other words, an ideal performance for ARR value would equal to 1. Fig. 3 shows experiment results by three descriptors (see Table 3 also). The ARR value of the conventional LBP is 0.788, whereas ARR of the HTD descriptor is 0.38 on our data set. Results indicate that the total average retrieval rate by the proposed method is improved significantly. We also examine the retrieval performance by ANMRR, where a low value represents high performance. The results are shown in Fig. 4. The ANMRR is 0.694 using the HTD and improved to 0.23 when proposed method is used. Again, the proposed descriptor has the best quantitative measure for retrieval rank.

We have noticed that the RLBP descriptor provides the best retrieval accuracy for most cases except "water", "Line" and "spot" for ARR, "water" and "spot" for ANMRR. From the viewpoint of human perception, the textures of water and desert are very similar with weak edge, please see Table 1. The proposed methods slightly degrade retrieval performance as compared with conventional LBP.

Experiment 2: Similarity retrieval for composite-texture In this experiment, we wish to test the retrieval performance of the proposed methods for the inhomogeneous textures. Consider the composite images shown in Table 2, each image consists of four different textures. The retrieval results with similarity by the three different methods are presented. By comparing the textures of the query and the matched images, it is clear that proposed descriptor has the best performance for matching similar textures. Overall, the proposed descriptor provides the best agreement with human perception, and most of the retrieved images have similar texture types with the query image. This experiment shows that the proposed method is able to distinguish composite images. On the other hand, the LBP

TABLE 4. The performance comparisons for different methods

Methods Classes	Co-LBP		HTD		Proposed method (Co-RLBP)	
	ARR	ANMRR	ARR	ANMRR	ARR	ANMRR
Class 1	0.97	0.03	0.72	0.429	0.99	0.013
Class 2	1	0.003	0.37	0.702	1	0
Class 3	0.93	0.084	0.42	0.654	0.96	0.053
Class 4	0.99	0.009	0.73	0.464	0.99	0.009
Class 5	0.93	0.094	0.89	0.32	1	0.027
Class 6	1	0.014	0.72	0.491	1	0.001
Class 7	0.99	0.012	0.49	0.652	1	0
Class 8	0.99	0.02	0.78	0.454	0.98	0.026
Class 9	0.97	0.038	0.99	0.115	0.99	0.024
Class 10	1	0	0.56	0.564	1	0
Average	0.977	0.03	0.667	0.484	0.991	0.015

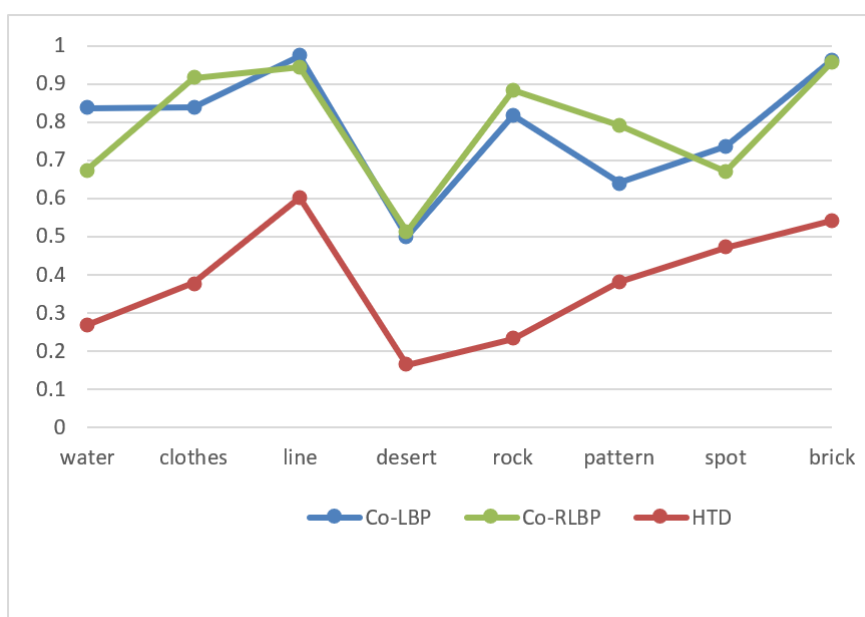


FIGURE 5. Comparisons with ARR for three methods

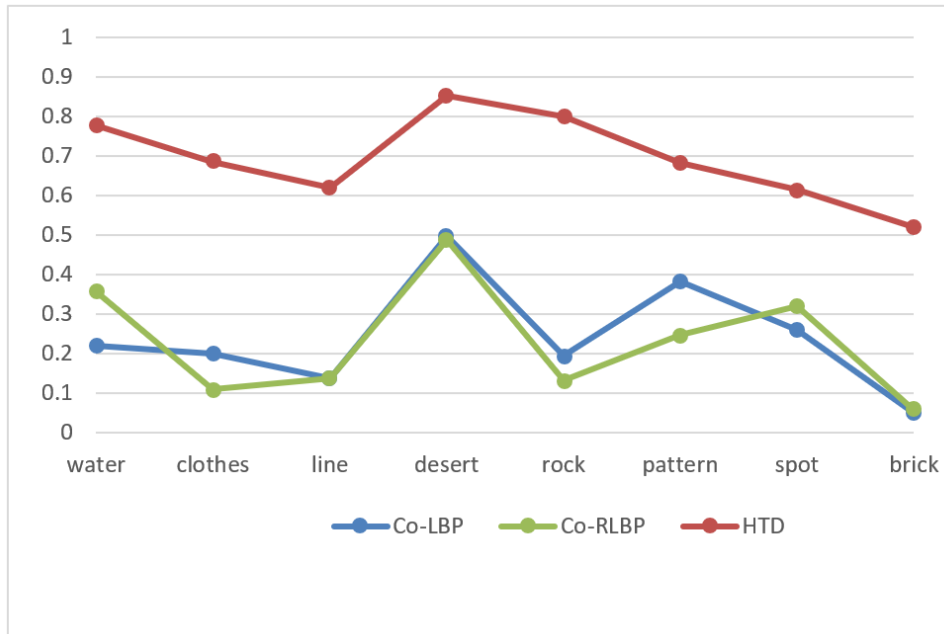


FIGURE 6. Comparisons with ANMRR for three methods

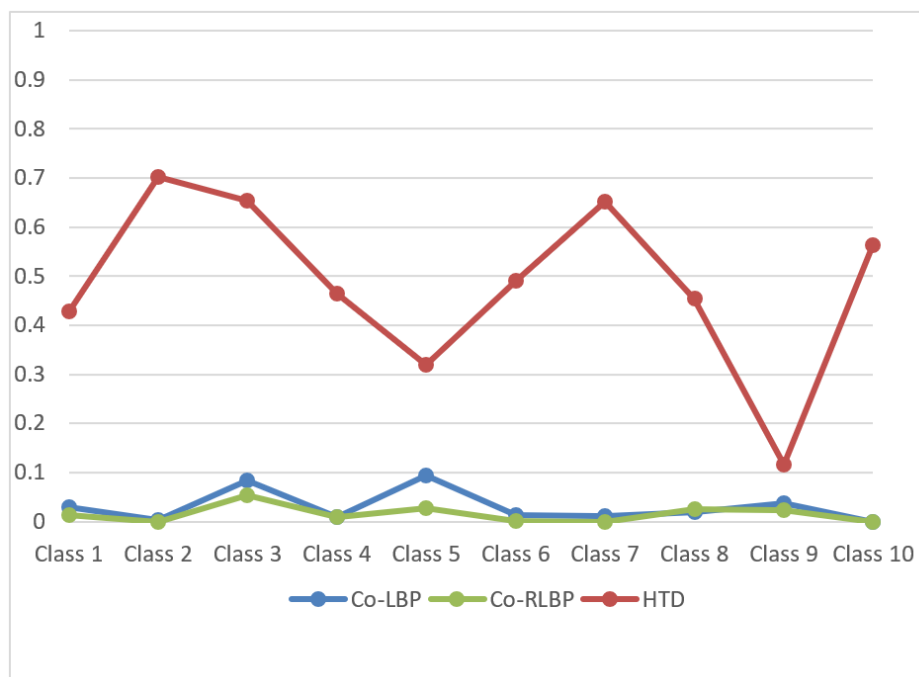


FIGURE 7. Comparisons with ANMRR for three methods

descriptor can also provide satisfactory results for this retrieval. Due to its simplicity, it makes possible for a very fast retrieval system with little degrade performance.

To test the retrieval accuracy, the evaluations by ARR and ANMRR are applied, again. As shown in Fig. 5 and 6 (also in Table 4), average ARR values by the methods of HTD, LBP and proposed descriptor are 0.667, 0.977 and 0.991; and average ANMRR values are 0.485, 0.03 and 0.015, respectively. Computed results indicate that the proposed descriptor provides the best retrieval accuracy for composite-texture retrieval.

5. **Conclusions.** In this paper, new descriptors for texture image retrieval have been proposed. The proposed texture descriptor is considered the texture pattern distribution. The new descriptor is not only robust for noise but also with strong spatial correlation, and it can effectively identify various image textures. Experimental results have proved that this method performs efficiently for texture similarity retrieval. In the future, we will continue to develop this research and try to apply to medical images analysis.

REFERENCES

- [1] M. Flickner et al. Query by Image and Video Content: The QBIC System , *IEEE computers* , vol. 28, pp. 23-32, 1995.
- [2] W. Y. Ma and B. S. Manjunath, Netra: A Toolbox for Navigating Large Image Database *in Proc. Int. Conf. on Image Proc.* 1, pp. 568-571, Santa Barbara, CA, 1997.
- [3] A. Pentland, R.W. Picard, and S. Sclaroff, Photobook. Tools for Content-based Manipulation of Image Database *International Journal of Computer Vision* , vol. 18, pp. 233-254, 1996.
- [4] J. Smith and S. Chang. VisualSEEK: A Fully Automated Content-based Image Query System *in Proc. ACM International Conference on Multimedia*, pp. 87-98, 1996.
- [5] R. M. Haralick, Statistical and structural approaches to texture, *Proc. IEEE*, vol. 67, no. 5, pp. 786-804, 1979.
- [6] C.M. Wu, Y.C. Chen, Statistical feature matrix for texture analysis, *Comput Vision Graph Images Process*, vol. 54, pp. 407-419, 1992.
- [7] T. Ojala, M. Pietikäinen, and David Harwood, A comparative study of texture measures with classification based on feature distributions, *Pattern Recognition*, vol. 29, no. 1, pp. 51-59, 1996.
- [8] T. Ojala, M. Pietikainen, and T. Maenpaa, Multiresolution gray-scale and rotation invariant texture classification with local binary patterns, *IEEE Transactions on Pattern Analysis and Machine Intelligence*, vol. 24, no. 7, pp. 971-987, 2002.
- [9] G. Schaefer and N. P. Doshi, Multidimensional local binary pattern descriptors for improved texture analysis, *in 21st IEEE International Conference on Pattern Recognition (ICPR)*, pp. 2500-2503, 2012.
- [10] J.F. Ren, X.D. Jiang, J.S. Yuan, Quantized fuzzy LBP for face recognition *2015 IEEE International Conference on Acoustics, Speech and Signal Processing (ICASSP)*, pp. 1503-1507, 2015.
- [11] N.H. Lu, C.M. Kuo, C.H. Liu , H.J. Ding, Liver Fibrosis Classification Based on Efficient Region of Interest Extraction in B-Mode Ultrasound Image *ICIC Express Letters, Part B: Applications*, vol. 4, no. 6, pp. 1565-1570, 2013.
- [12] D. K. Iakovidis, E. G. Keramidas and D. Maroulis, Ambiguous Local Binary Patterns for Ultrasound Texture Characterization, *CIAR* , vol. 5112, pp.750-759, 2008.